Supporting Information for

Trifunctional noble-metal-free multi-site electrocatalysts based on NiMn-LDH/$CuCo_2S_4$/rGO for energy-saving hydrogen generation via UOR/HER/OER

Reza Abazari,[a]* Joanna Goscianska,[b] Malek Naderi,[c,d]* Min Liu[e]* and Soheila Sanati[a]*

[a]*Department of Inorganic Chemistry, Faculty of Basic Sciences, University of Maragheh, P.O. Box 55181-83111, Maragheh, Iran. E-mails: reza.abazari@maragheh.ac.ir, s.sanati@stu.maragheh.ac.ir*

[b]*Faculty of Chemistry, Department of Chemical Technology, Adam Mickiewicz University, Uniwersytetu Poznańskiego 8, 61-614 Poznań, Poland*

[c]*Department of Materials and Metallurgical Engineering, Amirkabir University of Technology (Tehran Polytechnic), 1591634311 Tehran, Iran. Email: Mnaderi@aut.ac.ir*

[d]*Graphene and Advanced Materials Laboratory (GAMLab), Innovation tower of Amirkabir University of Technology (Tehran Polytechnic), 1591634311 Tehran, Iran*

[e]*Hunan Joint International Research Center for Carbon Dioxide Resource Utilization, State Key Laboratory of Powder Metallurgy, School of Physics, Central South University, Changsha 410083, P. R. China. E-mail: minliu@csu.edu.cn*

Characterization techniques: The powder x-ray diffraction (PXRD) patterns were recorded by a Bruker AXS model D8 advance diffractometer in Bragg angle from 5° to 65° with λ=1.54187 Å. The field emission scanning electron microscope (FE-SEM) images were performed using a FE-SEM ZEISS Sigma 300. The TEM image was investigated using the TEM Philips EM 208S instrument. To do EDAX analysis JEOL JSM-6380LV scanning electron microscope was applied. The Thermo-Scientific ESCALAB 250Xi was applied to analyze the surface elemental composition.

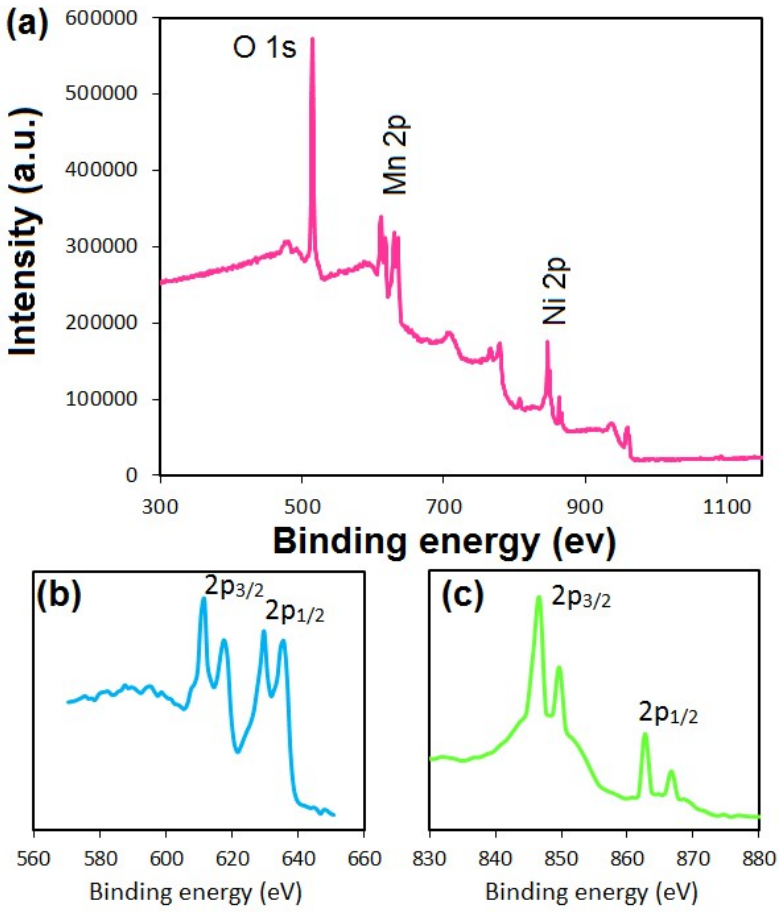

Figure S1. XPS survey spectrum of pristine NiMn-LDH (a), high-resolution XPS spectra of Ni 2p (b) and Mn 2p (c).

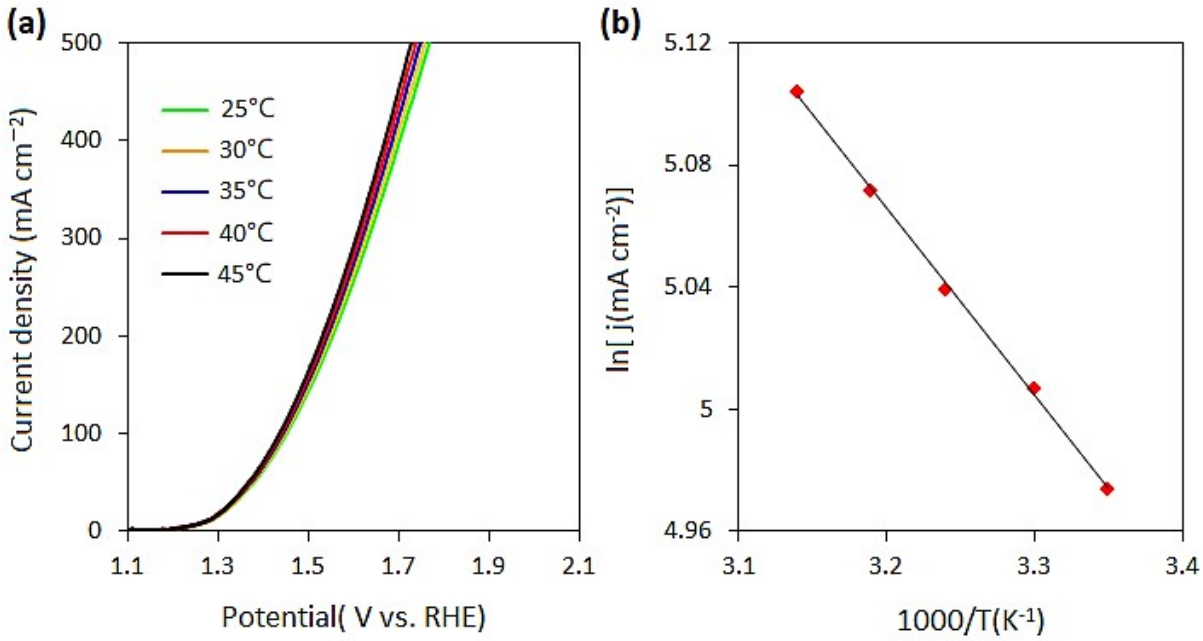

Figure S2. LSV curves of rGO/$CuCo_2S_4$/NiMn-LDH at different temperatures, (b) lni-1/T liner fitting curves for E_a in UOR.

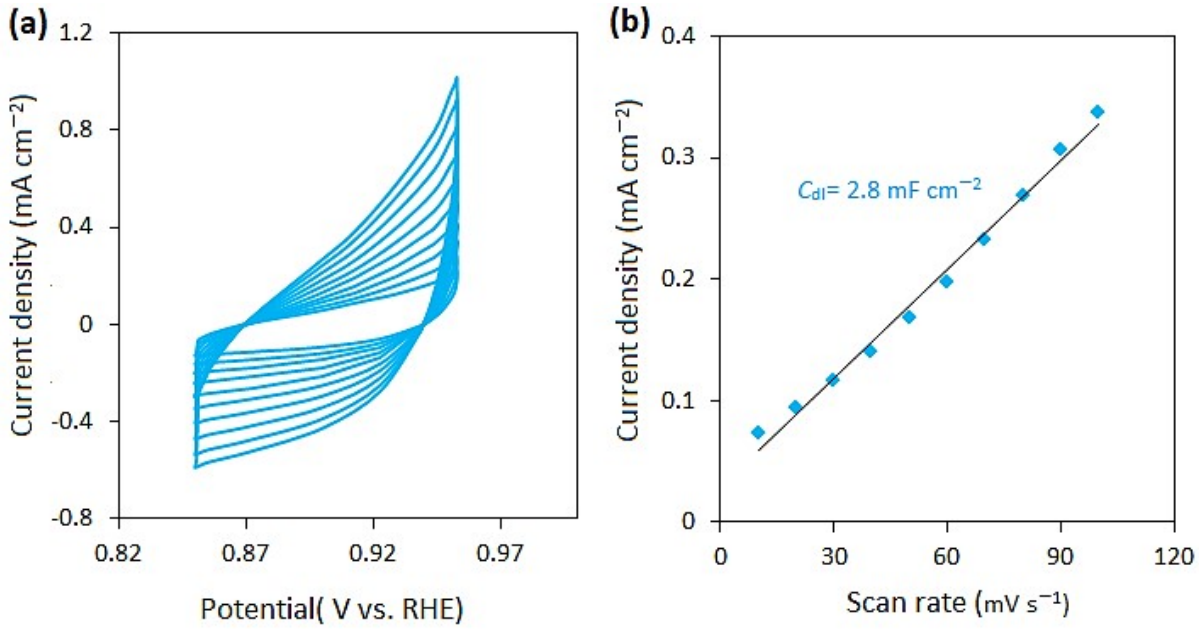

Figure S3. (a) CV curves of $CuCo_2S_4$ at different scan rates in UOR condition, (b) C_{dl} linear fitting curve.

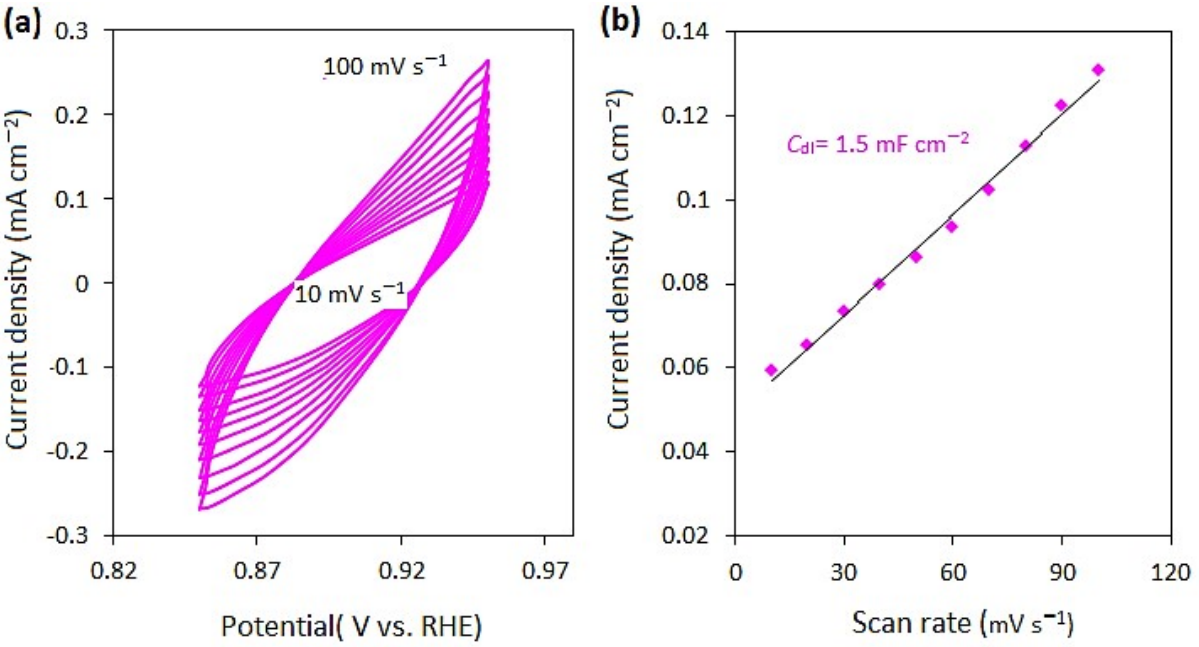

Figure S4. (a) CV curves of NiMn-LDH at different scan rates in UOR condition, (b) C_{dl} linear fitting curve.

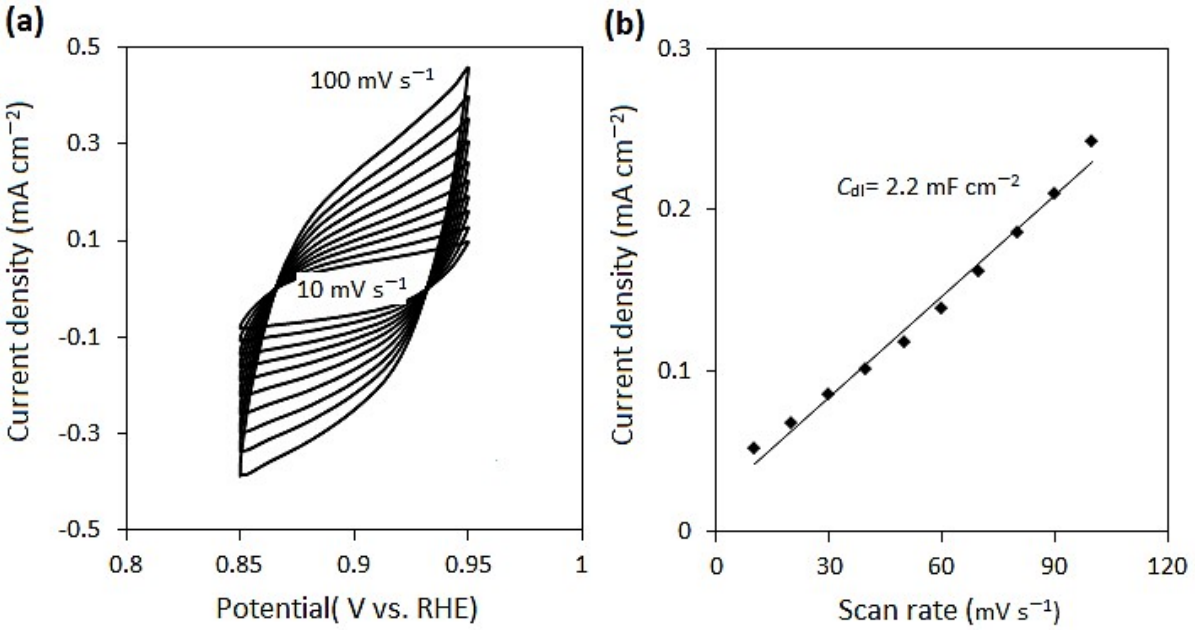

Figure S5. (a) CV curves of rGO at different scan rates in UOR condition, (b) C_{dl} linear fitting curve.

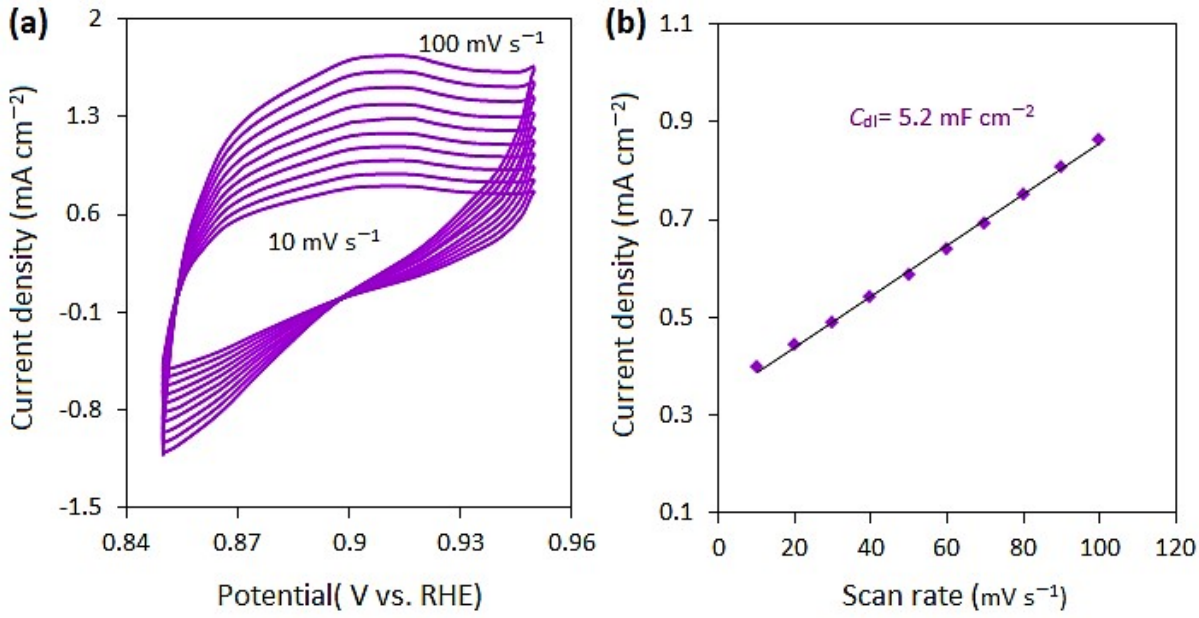

Figure S6. (a) CV curves of $CuCo_2S_4$/NiMn-LDH at different scan rates in UOR condition, (b) C_{dl} linear fitting curve.

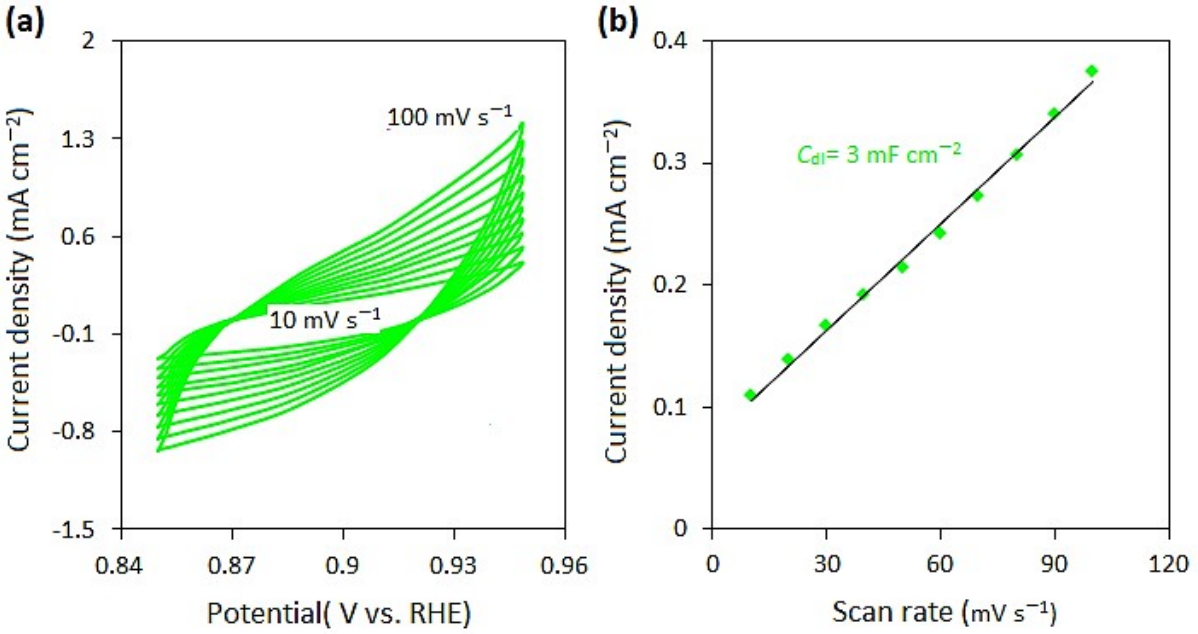

Figure S7. (a) CV curves of $CuCo_2S_4$/rGO at different scan rates in UOR condition, (b) C_{dl} linear fitting curve.

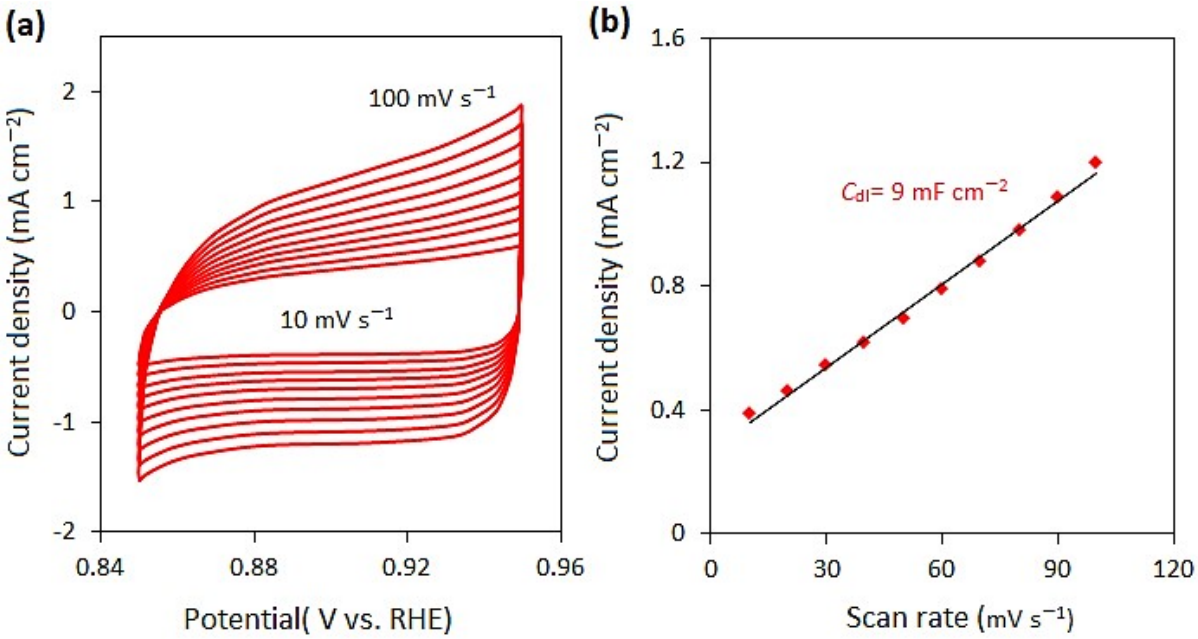

Figure S8. (a) CV curves of NiMn-LDH/$CuCo_2S_4$/rGO at different scan rates in UOR condition, (b) C_{dl} linear fitting curve.

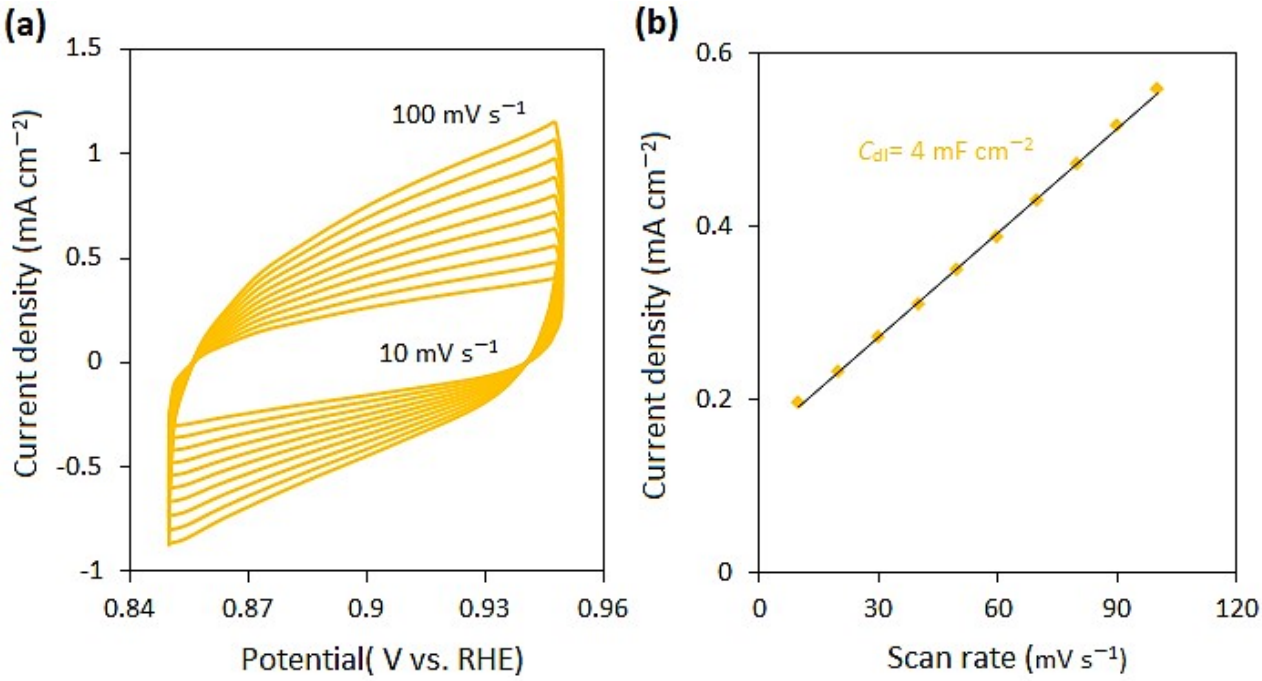

Figure S9. (a) CV curves of NiMn-LDH/rGO at different scan rates in UOR condition, (b) C_{dl} linear fitting curve.

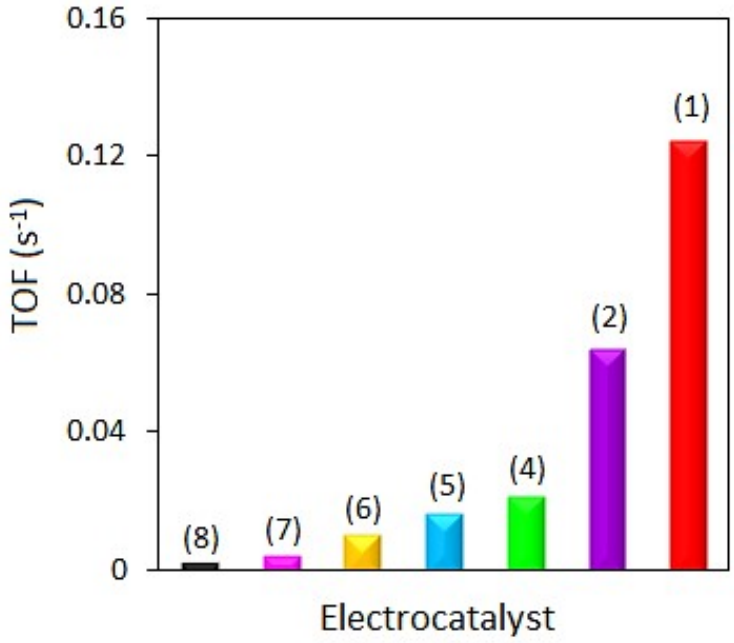

Figure S10. TOF amounts of the electrocatalysts: (1) NiMn-LDH/$CuCo_2S_4$/rGO, (2) NiMn-LDH/$CuCo_2S_4$, (4) $CuCo_2S_4$/rGO, (5) $CuCo_2S_4$, (6) NiMn-LDH/rGO, (7) NiMn-LDH, (8) rGO,

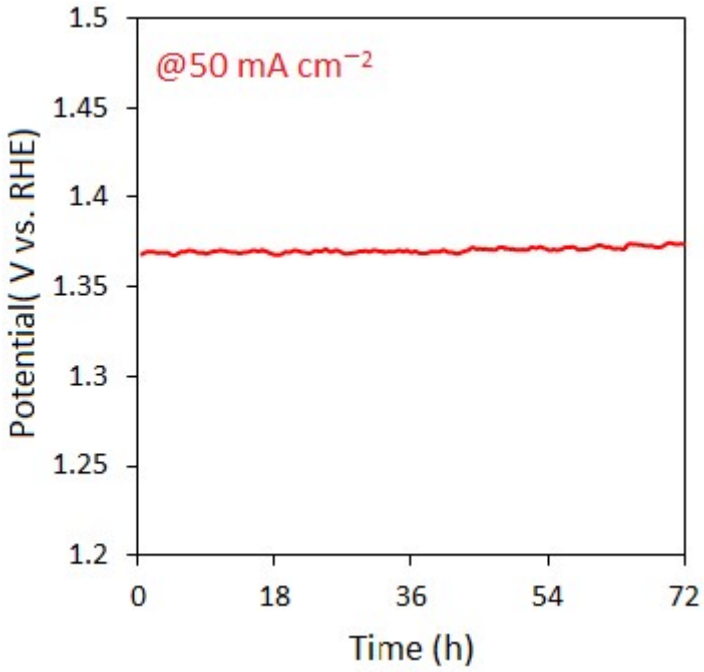

Figure S11. chronopotentiometric curve of NiMn-LDH/$CuCo_2S_4$/rGO in long period of time for UOR.

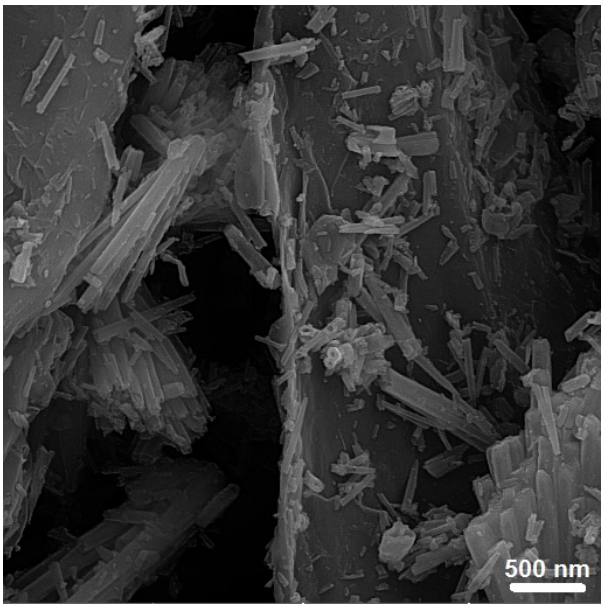

Figure S12. FE-SEM image of NiMn-LDH/$CuCo_2S_4$/rGO after UOR tests.

Table S1. OER performance of rGO/$CuCo_2S_4$/NiMn-LDH@NF in comparison with literature.

Electrocatalyst	Overpotential (mV@ 10 mA cm^{-2})	Reference
NiMn-LDHs (Br^-)	240	S1
NiFe LDH/NiS	230	S2
Ni_3Fe LDH	249	S3
FeNi LDH/$FeNi_2S_4$	259	S4
NiFeCe-LDH	232	S5
NiFe-LDH	281	S6
NiFe-LDH/SnS	310	S7
CoFeP/rGO-2	275	S8
Fe-doped $NiWO_4$	230	S9
NiMoO4/NF	310	S10
rGO/$CuCo_2S_4$/NiMn-LDH@NF	220	This work

Table S2. OER performance of electrocatalysts for OER.

Electrocatalyst	η_{10} (mV)	Tafel slope(mV dec^{-1})
RuO_2	218	126
$CuCo_2S_4$	308	199
NiMn-LDH	448	247
rGO	610	249
$CuCo_2S_4$/NiMn-LDH	244	173
$CuCo_2S_4$/rGO	277	195
NiMn-LDH/rGO	339	222
rGO/$CuCo_2S_4$/NiMn-LDH@NF	220	150

Table S3. Potential, Tafel slope, activation energy, double layer capacitance of electrocatalysts for UOR.

Electrocatalyst	Potential (v)@10 mA cm^{-2}	Tafel slope (mV dec^{-1})	C_{dl} (mF cm^{-2})
RuO_2	1.40	139	–
$CuCo_2S_4$	1.44	143	2.8
NiMn-LDH	1.58	153	1.5
rGO	1.71	155	2.2
$CuCo_2S_4$/NiMn-LDH	1.31	140	5.2
$CuCo_2S_4$/rGO	1.41	141	3
NiMn-LDH/rGO	1.47	150	4
rGO/$CuCo_2S_4$/NiMn-LDH@NF	1.27	136	9

Table S4. UOR performance of NiMn-LDH/$CuCo_2S_4$/rGO and the reported electrocatalysts.

Electrocatalyst	Potential/current density (V@mA cm^{-2})	Reference
LDH/α-FeOOH	1.35@10	S11
Mo-FeNi LDH	1.32@10	S12
$NiCoV_{1.0}$-LDH/NF-100	1.33@10	S13
NiCoCr-LDH/NF	1.38@100	S14
NiCo-LDH/NF	1.48@25	S15
Ni-TPA@NiSe/NF	1.37@100	S16
Mn-NiOOH	1.42@100	S17
CoNi-LDH/Fe MOF/NF	1.55@100	S18
FQD/CoNiLDH	1.36@10	S19
NiS/Ni_3S_2-Ni@NCNT	1.37@10	S20
rGO/$CuCo_2S_4$/NiMn-LDH@NF	1.27@10	This work

Table S5. HER performance of NiMn-LDH/$CuCo_2S_4$/rGO and the reported electrocatalyst

Electrocatalyst	Overpotential at 10 $mAcm^{-2}$ (mV)	Ref.
CoMnLDH@$Cu(OH)_2$/CF	155	S21
NiFe-LDH	245	S22
NiFe-LDH	272	S23
NiFe LDH-NS@DG hybrid	115	S24
Ni_5Fe LDH@NF	133	S25
NiCoFe LTHs/CFC	200	S26
CoSe/NiFe-LDH/EG	260	S27
NiFe-LDH/$NiCo_2O_4$/NF	257	S28
NiMn-LDH/$CuCo_2S_4$/rGO	101	This work

References

S1 S.A. Chala, M.C. Tsai, B.W. Olbasa, K. Lakshmanan, W.H. Huang, W.N. Su, Y.F. Liao, H. Lee, J.F. Dai, and B.J. Hwang, *ACS Nano*, 2021, **15**, 14996-15006.

S2 Q. Wen, K. Yang, D. Huang, G. Cheng, X. Ai, Y. Liu, J. Fang, H. Li, L. Yu, and T. Zhai, *Adv. Energy Mater*., 2021, **11**, 2102353.

S3 W. Jiang, A.Y. Faid, B.F. Gomes, I. Galkina, L. Xia, C.M.S. Lobo, M. Desmau, P. Borowski, H. Hartmann, A. Maljusch, A. Besmehn, C. Roth, S. Sunde, W. Lehnert, and M. Shviro, *Adv. Funct. Mater*., 2022, **32**, 2203520.

S4 J. Yuan, B. Huang, Y. Lu, H. Xu, Y. Qiao, H. Xu, G. He, and H. Chen, *Appl. Surf. Sci*., 2023, **610**, 155480.

S5 Y. Liao, R. He, W. Pan, Y. Li, Y. Wang, J. Li, and Y. Li, *Chem. Eng. J*., 2023, **464**, 142669.

S6 Y. Wang, Y. Gao, L. Ma, Y. Xue, Z. H. Liu, H. Cui, N. Zhang, and R. Jiang, *ACS Appl. Mater. Interfaces*, 2023, **15**, 16732–16743.

S7 Y. Sun, Q. Cai, Z. Wang, Z. Li, Q. Zhou, X. Li, D. Zhao, J. Lu, S. Tian, Y. Li, and S. Wang, *ACS Appl. Mater. Interfaces*, 2024, **16**, 23054–23060.

S8 X. Cai, Q. Song, D. Jiao, H. Yu, X. Tan, R. Wang, and S. Luo, *Int. J. Hydrogen Energy*, 2022, **47**, 39499-39508.

S9 H. N. Dhandapani, R. Madhu, A. De, M.A. Salem, B. R. Babu, and S. Kundu, *Inorg. Chem*., 2023, **62**, 11817–11828.

S10 A. Karmakar, K. Karthick, and S. Sankar, *J. Mater. Chem. A*, 2022, **10**, 17488.

S11 M. Cai, Q. Zhu, X. Wang, Z. Shao, L. Yao, H. Zeng, X. Wu, J. Chen, K. Huang, and S. Feng, *Adv. Mater*., 2023, **35**, 2209338.

S12 J.-M. Huo, Y. Wang, J.-N. Xue, W.-Y. Yuan, Q.-G. Zhai, M.-C. Hu, S.-N. Li, and Y. Chen, *Small*, 2024, **20**, 2305877.

S13 J. Guo, H. Zhang, Y. Yang, M. Wei, and H. Zhang, *J. Mater. Chem. A*, 2024, **12**, 16780-16792.

S14 S. Xu, D. Jiao, X. Ruan, Z. Jin, Y. Qiu, Z. Feng, L. Zheng, J. Fan, W. Zheng, and X. Cui, *Adv. Fun. Mater*., 2024, **34**, 2401265.

S15 K. Patil, P. Babar, H. Bae, E. Jo, J.-S. Jang, P. Bhoite, S. Kolekar, and J.-H. Kim, *Sustain. Energy Fuels*, 2022, **6**, 474-483.

S16 L. Jin, R. Ji, H. Wan, J. He, P. Gu, H. Lin, Q. Xu, and J. Lu, *ACS Catal*., 2023, **13**, 837–847.

S17 N. Duan, T. Hou, W. Zheng, Y. Qu, P. Wang, J. Yang, Y. Yang, D. Wang, J. Chen, and Q. Chen, *ACS Catal*., 2024, **14**, 1384–1393.

S18 Q.-N. Bian, B.-S. Guo, D.-X. Tan, D. Zhang, W.-Q. Kong, C.-B. Wang, and Y.-Y. Feng, *ACS Appl. Mater. Interfaces*, 2024, **16**, 14742–14749.

S19 Y. Feng, X. Wang, J. Huang, P. Dong, J. Ji, J. Li, L. Cao, L. Feng, P. Jin, and C. Wang, *Chem. Eng. J*., 2020, **390**, 124525.

S20 X. Guo, Y. Li, Z. Xu, D. Liu, A. Kong, and R. Liu, *Small*, 2025, **21**, 2408908.

S21 J. Wang, H. Yu, X. Wang, C. Chen, S. Li, N. Cai, W. Chen, Y. Xue, H. Li and F. Yu, *J. Indust. Eng. Chem*. 2022, **105**, 427-434.

S22 Y. Zhou, Z. Wang, Z. Pan, L. Liu, J. Xi, X. Luo and Y. Shen, *Adv. Mater*. 2019, **31**, 1806769.

S23 P. Zhai, M. Xia, Y. Wu, G. Zhang, J. Gao, B. Zhnag, S. Cao, Y. Zhang, Z. Li, Z. Fan, C. Wang, X. Zhang, J.T. Miller, L. Sun and J. Hou, *Nat. Commun*. 2021, **12,** 4587.

S24 Y. Jia, L. Zhang, G. Gao, H. Chen, B. Wang, J. Zhou, M. T. Soo, M. Hong, X. Yan, G. Qian and X. Yao, *Adv. Mater*. 2017, **29**, 1700017.

S25 Y. Zhang, Q. Shao, Y. Pi, J. Guo and X. Huang, *Small* 2017, **13**,1700355.

S26 A.-L. Wang, H. Xu and G.-R. Li, *ACS Energy Lett*. 2016, **1**, 445.

S27 Y. Hou, M. R. Lohe, J. Zhang, S. Liu, X. Zhuang and X. Feng, *Energy. Environ. Sci*. 2016, **9**, 478.

S28 Z. Wang, S. Zeng, W. Liu, X. Wang, Q. Li, Z. Zhao and F. Geng, *ACS Appl. Mater. Interfaces* 2017, **9**, 1488.